

EXPERIMENTAL INVESTIGATION OF THE EFFECT OF POWER UPON
THE STATIC LONGITUDONAL STABILITY OF A LOW WINGED
MONOPLANE AND A METHOD FOR ITS CALCULATION

Thesis by

M. K. Fleming, Jr.

In partial fulfillment of the requirements for
the Degree of Master of Science in Aeronautical Engineering

California Institute of Technology
Pasadena, California
1936

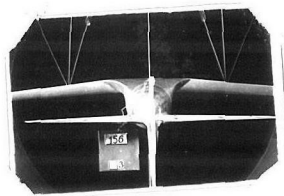
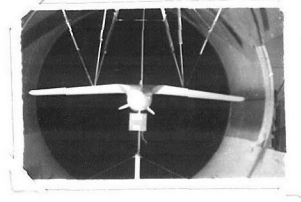
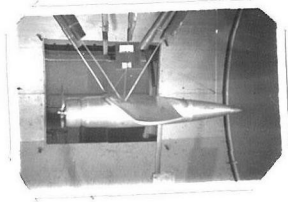
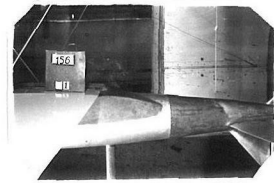
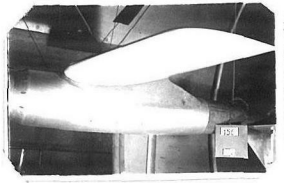
ACKNOWLEDGMENT

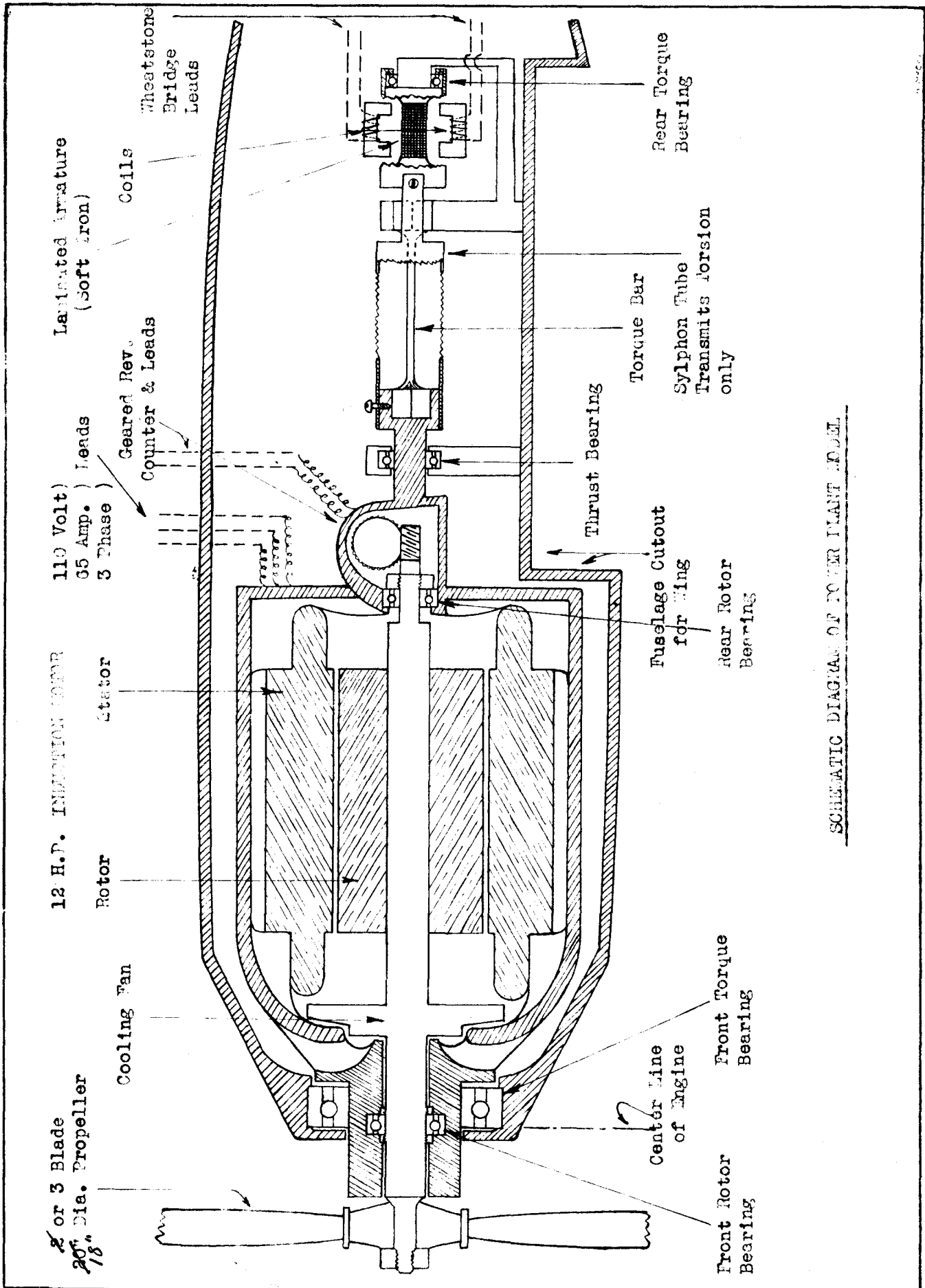
I wish to express my sincere appreciation of the constructive criticism given by Dr. Clark B. Millikan during the experimental and analization of data periods.

My gratitude is extended to Lieut.- Cmdr. Calvin Bolster, U.S. Navy, for his ceaseless efforts to make the model behave, and aid in compiling the original experimental results.

The willing cooperation of the aerodynamical departments of the Lockheed Aircraft Corporation and the Douglas Aircraft Company with regard to flight test data made possible the application of the results. -

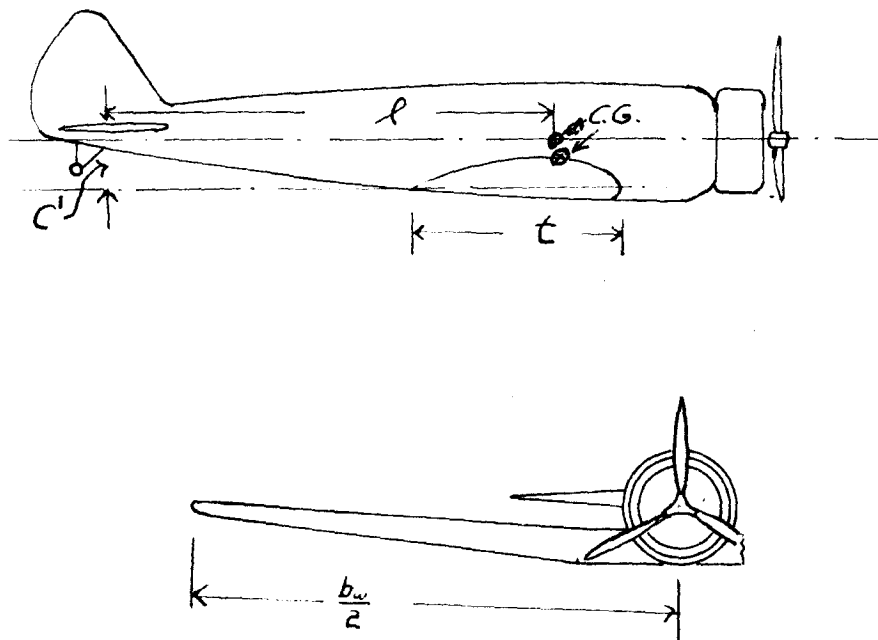
VIEWS OF MODEL
IN
WIND TUNNEL





SCHEMATIC DIAGRAM OF POWER PLANT MODEL

FIGURE 7.



FULL SCALE

$W = 5000^*$
 $BHP = 550$
 $e = .89$
 $f = 6.59$
 $\eta = .825$
 $\Omega = 5.89$
 $\beta = 29^\circ @ .75 R$
 $i_w = 0^\circ$
 $\alpha = +2^\circ$
 $R_w = 5.97$
 $R_T = 4.07$
 AIRFOIL - CLARK Y

MODEL

Dia. Prop = 18"
 $t = 1.211 \text{ ft.}$
 $\frac{b}{t} = \cancel{.10} \rightarrow .09$
 $b(\text{span}) = 5.75 t^2$
 $\frac{h}{t} = .25$
 $\frac{d}{t} = .30$
 $\frac{c'}{t} = .15$ (AVE. chord in front of tail)
 $S_{wA} = S' = 5.57 t^2$
 $S'_c = 1.14 t^2$
 $l = 3.22 \text{ ft.}$

Fig. 2

OBJECTIVE OF THIS EXPERIMENT

To obtain the change in the longitudinal moment of a low winged monoplane caused by the addition of the propulsive unit operating at various conditions of power.

To construct possible working charts for use in calculating this change from power off wind tunnel tests of scale models.

DESCRIPTION OF APPARATUS

The G.A.L.C.I.T. propeller powered model was used for the tests made in this investigation. The model was complete with fuselage, wings, tail surfaces, N.A.C.A. Cowl, three bladed propeller, electric motor.

The motor was a 12 H.P. electric motor rated at 12000 r.p.m. Since the model was one-sixth full scale the full scale power was $36 \times 12 = 432$ H.P. This was approximately the full power of the low-winged ^{Northrop} monoplane Alpha, with which the model was nearly geometrically similar. The propeller blade sections were of the same form as the Hamilton Standard 1A1-0, 20" Blade with tips cut to 18".

The torque, r.p.m. were measured according to the following description. The schematic diagram is shown in Figure 1 and the timing circuit in Figure 3.

The torque developed by the propeller is opposed in equal amount by the resisting moment in twist by the torque bar. A soft iron bar mounted on the torque bar and operating between the pole faces of coils (1) and (2) moves with the twist of the torque bar, varying their impedance. The change in impedance is indicated by balancing the bridge by means of the variable resistance. A calibration curve of a known torques and their corresponding resistance readings was made before and after each run, and the mean values

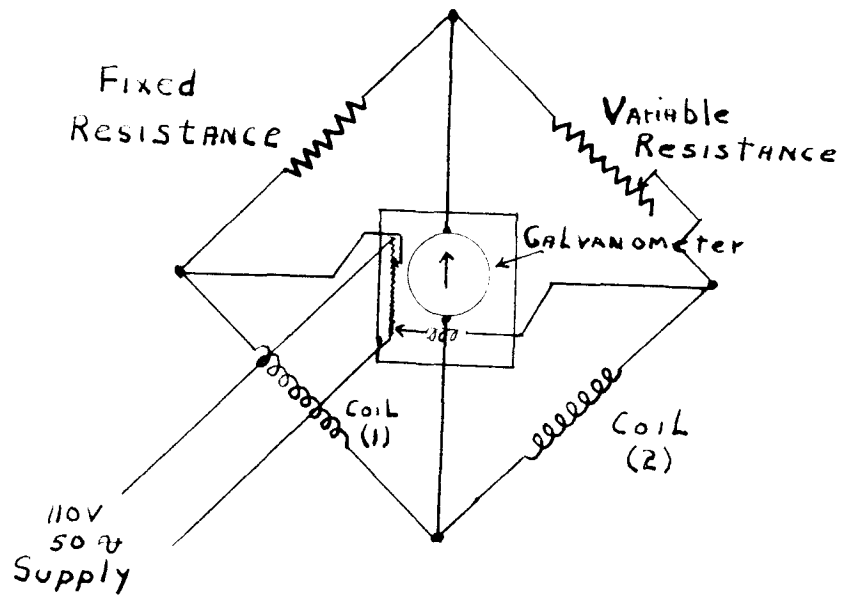
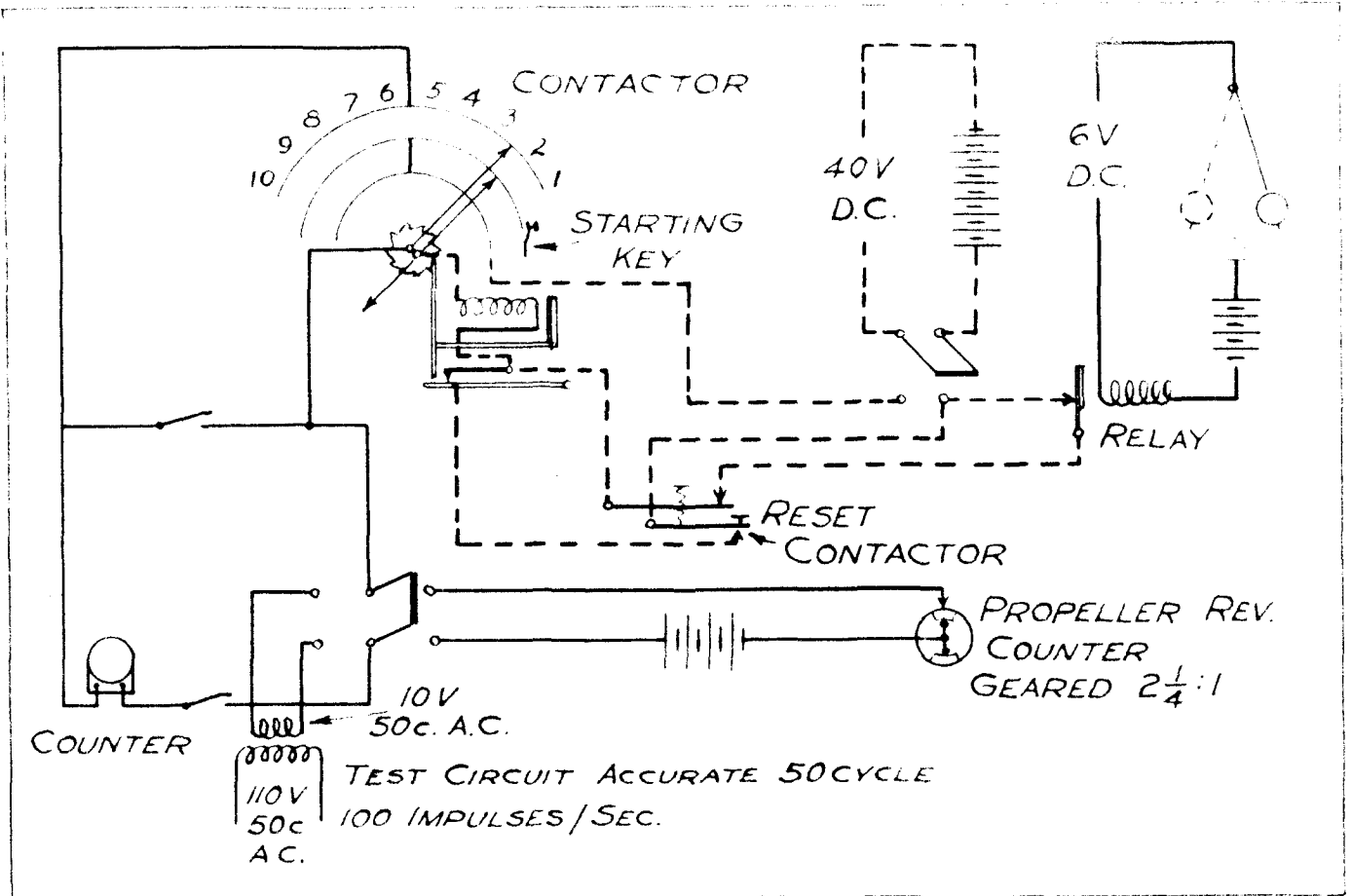


Fig. 3.

used. The resistance readings for balance of the bridge were then converted to kilogram-meters by the calibration curve. For calibration, known weights were placed on pans suspended by knife edges to the ends of a 50 cm. bar mounted on the stator.

A revolution counter was geared to the rotor and leads from the contactors were introduced into the timing circuit. This multiple relay circuit was actuated by a pendulum and the number of contacts were counted by an impulse counter over a period of approximately 10 seconds. The timing circuit was calibrated against a crystal controlled 50 cycle current several times during each run to obtain timing intervals. The quantities angle of attack, drag, lift and moments were measured in the normal manner by the G.A.L.C.I.T. six component balance system.

THEORY PERTAINING TO LONGITUDONAL STATIC STABILITY FOR UNACCELERATED RECTILINEAR FLIGHT

The development of the charts in this paper as well as the method of attack upon the problem was based upon the theoretical treatment of longitudinal static stability by Dr. C. B. Millikan in his course of aerodynamics at Calif. Ins. of Tech.

The most suitable method of indicating the degree of power for airplanes in unaccelerated rectilinear flight is the power parameter (θ) developed by Millikan and is equal to the negative of the resultant drag divided by the lift. Its development is herewith repeated:

ANALYSIS OF THE EFFECT OF POWER ON LIFT, DRAG, AND PERFORMANCE

In order to give a satisfactory discussion of this subject, it is necessary to analyze the problem somewhat more closely than is customary. With

this in view, let us consider an airplane in climbing (or gliding) unaccelerated flight. The forces acting in the direction of the flight path may be split up into a thrust, T , a drag, D , and a gravity force as shown in Fig. 4.

The equilibrium condition is

$$D + W \sin \theta = T \tag{1}$$

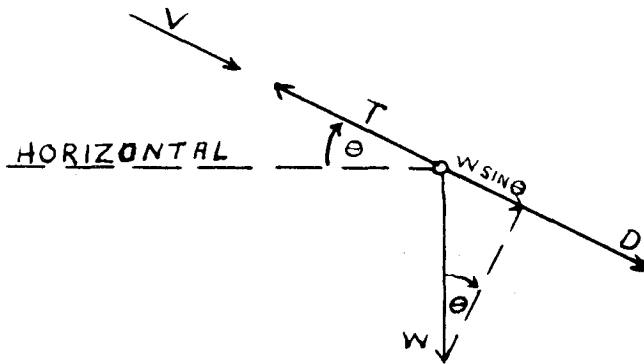


Fig. 4.

The precise definition of D and T has not yet been given. However, before discussing this question, let us first transform Eq. (1) to a more familiar and convenient form. Multiplying by V , expressing T in terms of brake horsepower P , and a propeller efficiency η' , and introducing the drag coefficient, C_D , we obtain:

$$C_D (\alpha, J) \rho S V + W \sin \theta V = P \eta' (\alpha, J) \tag{2}$$

where the variables upon which C_D and η' may depend have been explicitly indicated in parentheses. It will be noted that Eq. (2) is just the usual performance equation.

We have just stated that the precise significance of D and T in Eq. (1) had not yet been given. This means that in Eq. (2), C_D and η' have not yet

been exactly defined. Actually we may define either one in a rather arbitrary fashion, the other is then determined by the fact that the forces must be in equilibrium, i.e. Eq. (2) must be satisfied.

It has been customary in the past to define $C_D(\alpha, J)$ by equating it to $C_D(\alpha)$ which is the drag coefficient of the airplane without propeller. Then in order that Eq. (2) may be satisfied, the propeller efficiency $\eta'(\alpha, J)$ should be replaced by a propulsive efficiency $\eta(\alpha, J)$ determined from wind tunnel tests on an airplane or model with propeller running, and for all pertinent values of J and α . Eq. (2) would then take the form

$$C_{D_0}(\alpha) \rho S V + W \sin \Theta V = P \eta(\alpha, J) \quad (3)$$

Practically all propulsive efficiency investigations in the past have been restricted to the case of zero inclination of the thrust axis, so that the dependence of η on J is well known, while its dependence on α has been very little discussed. It was one of the essential aims of the present series of tests^{*} to furnish data on this variation of propulsive efficiency with thrust axis inclination. The data so obtained could be presented in the form of a series of normal propulsive efficiency charts each corresponding to a definite value of α or thrust axis inclination. However, the complications introduced into normal performance calculations, through the necessity of using such a family of propulsive efficiency charts, would be so overwhelming that it is very doubtful whether the data would be of any practical service. An entirely different method of presenting the results, based on a rather different point of view with respect to the performance equation is here suggested and gives the data in such a form that the designer can use them in performance estimation without any essential modification to the normal calculation procedure.

* See RUSSELL, McCoy, MILLIKAN PAPER No. 3 VOL. 3, J. of I.R.S.

In introducing this new method we return to Eq. (2) and replace $\eta'(\alpha, J)$ by a propulsive efficiency $\eta_0(J)$ which is determined from measurements at zero inclination of the thrust axis, i.e. η_0 is just the propulsive efficiency which is customarily given in the standard propeller charts. Then in order that Eq. (2) may be satisfied, we must replace C_D by an effective drag coefficient, C_{D_e} so that the performance equation now takes the form:

$$C_{D_e}(\alpha, J) \rho S V + W \sin \Theta V = P \eta_0(J) \quad (4)$$

(Note that at zero inclination of the thrust axis, Eqs. (3) and (4) are identical, i.e., $\eta = \eta_0$ and $C_{D_e} = C_{D_0}$). With this equation, performance is calculated in exactly the normal manner, using the standard propulsive efficiency charts, the only modification being that C_{D_e} is used instead of C_{D_0} . We shall return later to the discussion of how this modification is accomplished and shall see that no considerable additional labor is required. We must first, however, investigate the manner in which C_{D_e} may be determined from our wind tunnel tests.

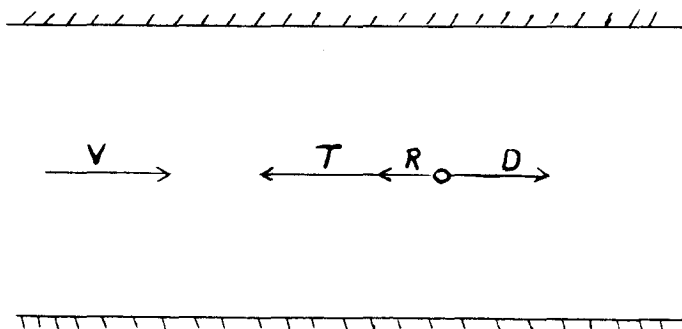


Fig. 5

In Fig. 5 the forces, in the direction of the relative wind, which act on the model mounted in the wind tunnel are indicated. R is the resultant force exerted by the model on the drag rigging, taken as positive in the direction of the drag force. Hence the external force which the drag rigging

exerts on the model is R , taken as positive in the direction of the thrust. The diagram, which has been drawn with all forces positive, is exactly analogous to the previous free-flight diagram, Fig. 4, except that the wind-tunnel diagram corresponds to a case in which $T < D$, i.e. to an airplane in gliding rather than climbing flight. The condition that the forces be in equilibrium leads to the equation

$$D = T + R,$$

or multiplying by V and defining the drag coefficient and propulsive efficiency exactly as in Eq. (4):

$$C_{D_e}(\alpha, J) \rho S V^2 - R V = P \eta_o(J) \quad (5)$$

Comparing with Eq. (4), we see that the wind tunnel and free-flight equations are identical if

$$R = -W \sin \theta \quad (6)$$

This means that the resultant force exerted by the drag balance on the model plays exactly the same role in the wind tunnel as does the component of the gravity force along the flight path in unaccelerated free flight. If we determine values of C_{D_e} in the wind tunnel for a series of values of R , the former are identical with the values of C_{D_e} in free flight for the corresponding values of $W \sin \theta$.

It appears now that we must determine C_{D_e} as a function of three independent parameters α , J , and R . However, it is easy to see that only two are independent. Dividing Eq. (5) by $\rho S V$ and introducing the coefficient of resultant force $C_R = R/S$ we obtain

$$(6)$$

$$C_{Dc}(\alpha, J) = C_R + F \eta_0 / \rho S V$$

But, at a given α , C_R is a function only of J , i.e., $J = J(\alpha, C_R)$. Hence, introducing torque and revolutions per second,

$$C_{Dc}(\alpha, C_R) = C_R + 2\pi Q \eta_0(J) / \rho S V$$

It is convenient to replace the variable α by the lift coefficient C_L since the latter is the essential parameter in the free flight case. If we define the lift as the resultant aerodynamic force perpendicular to V (including any contribution from inclined thrust), then the wind tunnel measurements give $\alpha = \alpha(C_L)$, (cf. Fig. 8). Hence we obtain the final equation for the determination of C_{Dc} :

$$C_{Dc}(C_L, C_R) = C_R + 2\pi Q \eta_0(J) / \text{Dia.} \rho S V \quad (7)$$

C_L , C_R , Q , ρ , and J are measured in the wind tunnel, Dia. and S are known, and $\eta_0(J)$ is obtained from propulsive efficiency charts corresponding to zero thrust inclination.

It now only remains to express C_R in terms of a parameter having a significance in free flight. If we follow the definition given above and take L as the resultant aerodynamic force perpendicular to the relative wind (flight path), then we see from Fig. 4. that for unaccelerated, rectilinear flight

$$L = W \cos \theta.$$

Combining with Eq. (6)

$$R / L = - \tan \theta.$$

or finally

$$C_R = - C_L \tan \theta. \quad (8)$$

Hence our wind tunnel observations finally give

$$C_{D_e} = C_{D_e}(C_L, \theta) \quad (9)$$

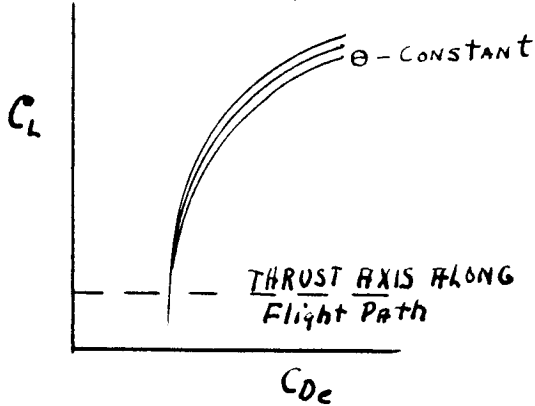


Fig. 6

The results may then be expressed in the form of a family of polars of C_{D_e} vs C_L , each polar corresponding to a constant angle of climb (or glide) θ . θ , then, is the parameter which represents the power condition of the model. These polars will have somewhat the character of those in Fig. 6, possessing a common intersection at the C_L corresponding to zero thrust axis inclination, which will normally be near the high speed attitude of the airplane.

We return finally to the question of how such data can most easily be used in performance analyses. Following Oswald (N.A.C.A. Tech. Rep. No. 408) we may define the airplane efficiency factor e by the equation

$$C_{D_e} = \frac{C_L^2}{e\pi AR} + C_{D_p} \quad (10)$$

(A.R. = aspect ratio = b^2/S , and C_{D_p} = parasite drag coefficient)

where e is chosen so as to determine as nearly a constant value of C_{D_p} as is possible over the flying range. Now since all of the polars will normally intersect close to the axis, $C_L = 0$, C_{D_p} will be practically the same for all, and the effect of variations in θ can be taken into account by varying e

only. This means that we may present all of the wind tunnel data pertinent to normal performance calculations by giving

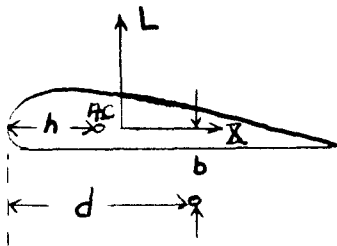
$$e = e(\theta). \quad (11)$$

Performance calculations may then be carried out in the conventional manner except that for any particular angle of climb the appropriate value of e , and hence of span loading, must be taken.

Before proceeding to a discussion of the experimental results in the light of the above considerations, it might be pointed out that angle of climb as introduced above appears to be the most satisfactory dimensionless parameter which can be found for describing the condition of power output under which an airplane is operating. Not only the performance characteristics of this section, but also the stability and control results of the next are presented in terms of this convenient parameter

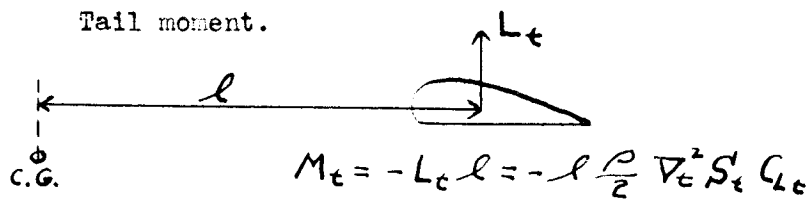
The following development of the static longitudinal moment is presented:

The moment due to the wing and fuselage is equal to



$$C_{M_{W.R.}} = C_{M_0} + \left[\left(\frac{d}{c} - .1 \frac{b}{c} - \frac{h}{c} \right) \right] C_L + \Delta C_M$$

Where ΔC_M is the additional moment due to the fuselage and C_{M_0} is the moment of the wing about its A.C. "b" is positive when the center of gravity is below the A.C. Clockwise moments are positive. $\left[\frac{d}{c} - .1 \frac{b}{c} \right]$ is the effective position of the center of gravity horizontally.



Define $C_{M_t} = \frac{M_t}{\frac{\rho}{2} V^2 S_w t} = - \frac{l S_t V_t^2}{t S_w V^2} C_{L_t}$

Where "t" is the mean aerodynamic chord of the wing. S_t is the area of horizontal tail surfaces. V_t is the velocity of the air over the tail.

$\frac{l S_t}{t S_w}$ is known as the tail-wing volume ratio.

$$\therefore C_{M_t} = - \frac{V_t^2}{V^2} \frac{l S_t}{t S_w} C_{L_t}$$

$$V_t < V \quad \therefore \text{Let } \eta_t = \frac{V_t^2}{V^2}$$

$$C_{M_t} = - \eta_t \frac{l S_t}{t S_w} C_{L_t}$$

(1)

$$\begin{aligned} C_{L_t} &= a_0 \alpha_{o_t} = a_0 (\alpha_t - \text{Downwash angle}) \\ &= a_0 (\alpha_w - \alpha_d - \epsilon_t - \epsilon_w) \end{aligned}$$

Where $\alpha_d = \alpha_w - \alpha_t$ (α_w and α_t measured from zero lift)

ϵ_t is downwash due to tail

ϵ_w is downwash due to wing

Assuming elliptical lift distribution

$$\epsilon_t = \frac{C_{L_t}}{\pi A R_t}$$

Letting $\epsilon_w =$ twice downwash at wing

$$\epsilon_w = \frac{2 C_{L_w}}{\pi A R_w}$$

(10)

Then

$$C_{L_t} = a_0 \left(\alpha_{0w} - \frac{C_{L_w}}{\pi A_w} - \frac{C_{L_w}}{\pi A_w} - \frac{C_{L_t}}{\pi A_t} - \alpha d \right)$$

Collecting

$$C_{L_t} \left(1 + \frac{a_0}{\pi A_t} \right) = C_{L_w} \left(1 - \frac{a_0}{\pi A_w} \right) - a_0 \alpha d$$

$$C_{L_t} = \left(\frac{1 - \frac{a_0}{\pi A_w}}{1 + \frac{a_0}{\pi A_t}} \right) C_L - \left(\frac{a_0}{1 + \frac{a_0}{\pi A_t}} \right) \alpha d$$

(2)

Putting (2) in (1)

$$C_{M_t} = -\eta_t \frac{L S_t}{t S_w} \left[\frac{1 - \frac{a_0}{\pi A_w}}{1 + \frac{a_0}{\pi A_t}} C_L - \frac{a_0}{1 + \frac{a_0}{\pi A_t}} \alpha d \right]$$

GENERAL EFFECTS OF POWER

The effects of power on the wings are:

The visual effects of power on the flow over the wings as viewed in the smoke tunnel of the N.A.C.A. at Langley Field showed,

- 1) Increase of velocity over the wings.
- 2) Delaying of the separation to higher angles of attack.

Increasing the velocity increases the parasite drag, induced drag and the lift for the same angle of attack. The delaying of separation increases the angle of stall.

The probable effects of power on the tail (based on power off formulae) are:

In the development of the tail moment coefficient two assumptions are made.

- a) Elliptical lift distribution.
- b) Downwash due to the wing at the tail is twice the downwash of the wing.

The lift distribution is generally not elliptical, which is one small error. The downwash at the tail due to the wing with power on or power off has not been proven to be that assumed.

For an untwisted wing any error in (a) should give a constant error, while change in downwash may give a varying effect with power. The latter will give an effective change in the tail efficiency η_t .

- c) η_t will absorb changes in velocity over the tail due power.

Therefore, if power increases the velocity over the tail, η_t should become larger.

Now if C_{M_c} power off and power on are compared at same C_L then the only changes in η_t will be for (c) which is known to increase with power, and additional change in downwash angle.

TESTING PROCEDURE

The testing procedure is essentially the same as that used by Russell and McCoy, and fully described in the Journal of the Institute of Aeronautical Sciences, January, 1936, issue. A brief outline follows.

The standard wind tunnel testing procedure plus the addition of the torque and revolution counter apparatus will give all the necessary data for evaluating C_M , C_L , C_R , T_{AND} , for various angles of attack and elevator angles, provided that a typical airplane to which the model conforms is selected and a traverse of the area between the power available and the power required curves is made.

The typical airplane selected was the Northrop Alpha since it was very nearly geometrically similar to the model. See figure No. 2 for diagram

Full Scale Airplane Power Curves

HP
500

Power Available \neq Power Required, Full Scale

Assumptions: -

$$W = 5000 \text{ lb}, R_{w} = 17.05$$

$$l_s = 3.23 \quad l_p = 7.58 \quad l_t = 11.02$$

400

300

200

100

THP_a

THP_r

V_s

50

65

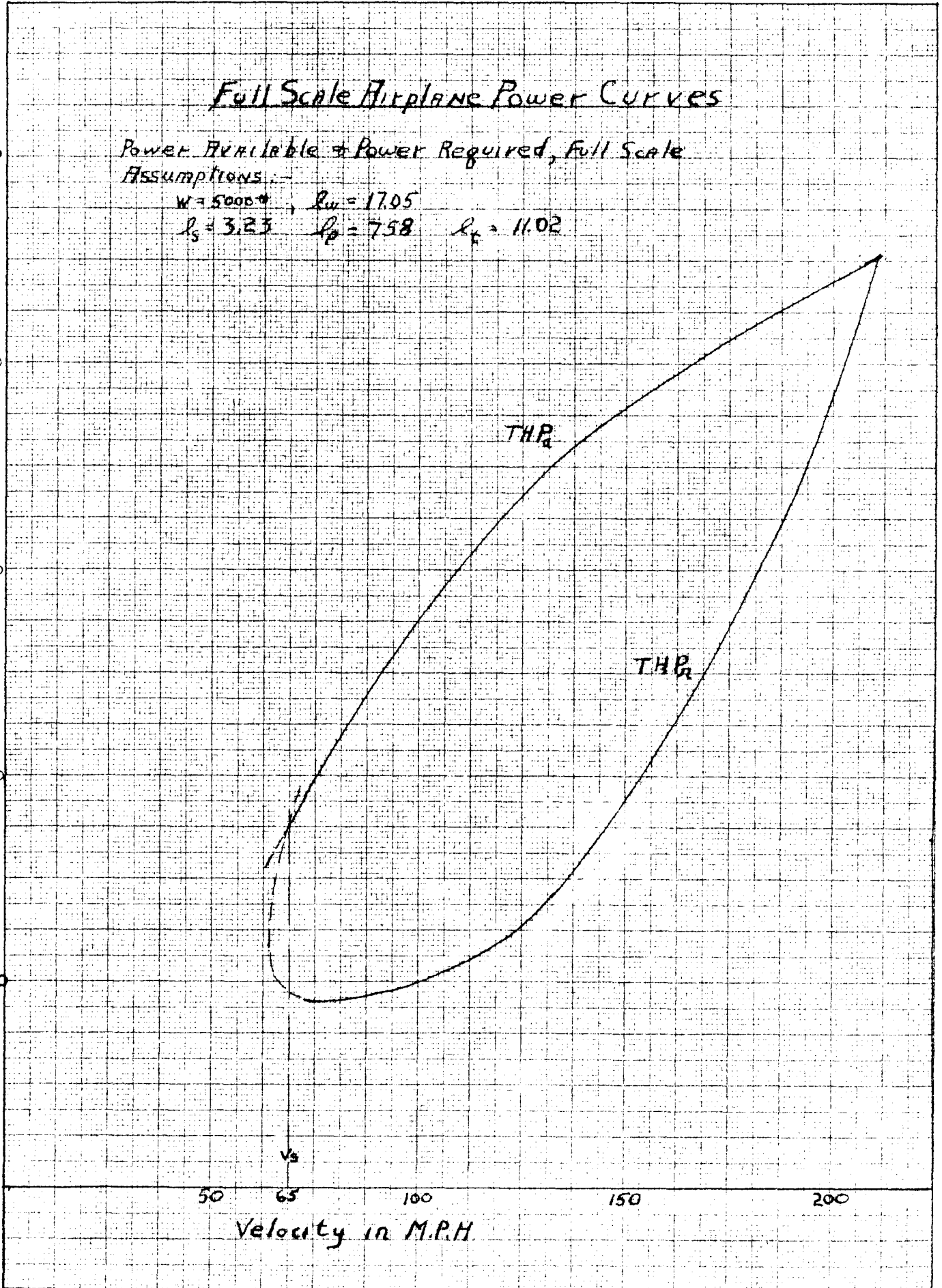
100

150

200

Velocity in M.P.H.

Fig. 7.



Thrust Horsepower Available & Required
 Values of Y_{HT} , α_{HT} & Wind Tunnel "g"
 for performance of Power Model
 under following Assumptions

$\rho_p = 758$

$W = 5000 \#$ $\rho_w = 17.05$

$\rho_s = 3.23$ $R_p = 11.02$

⑤ indicate r.p.s. of propeller

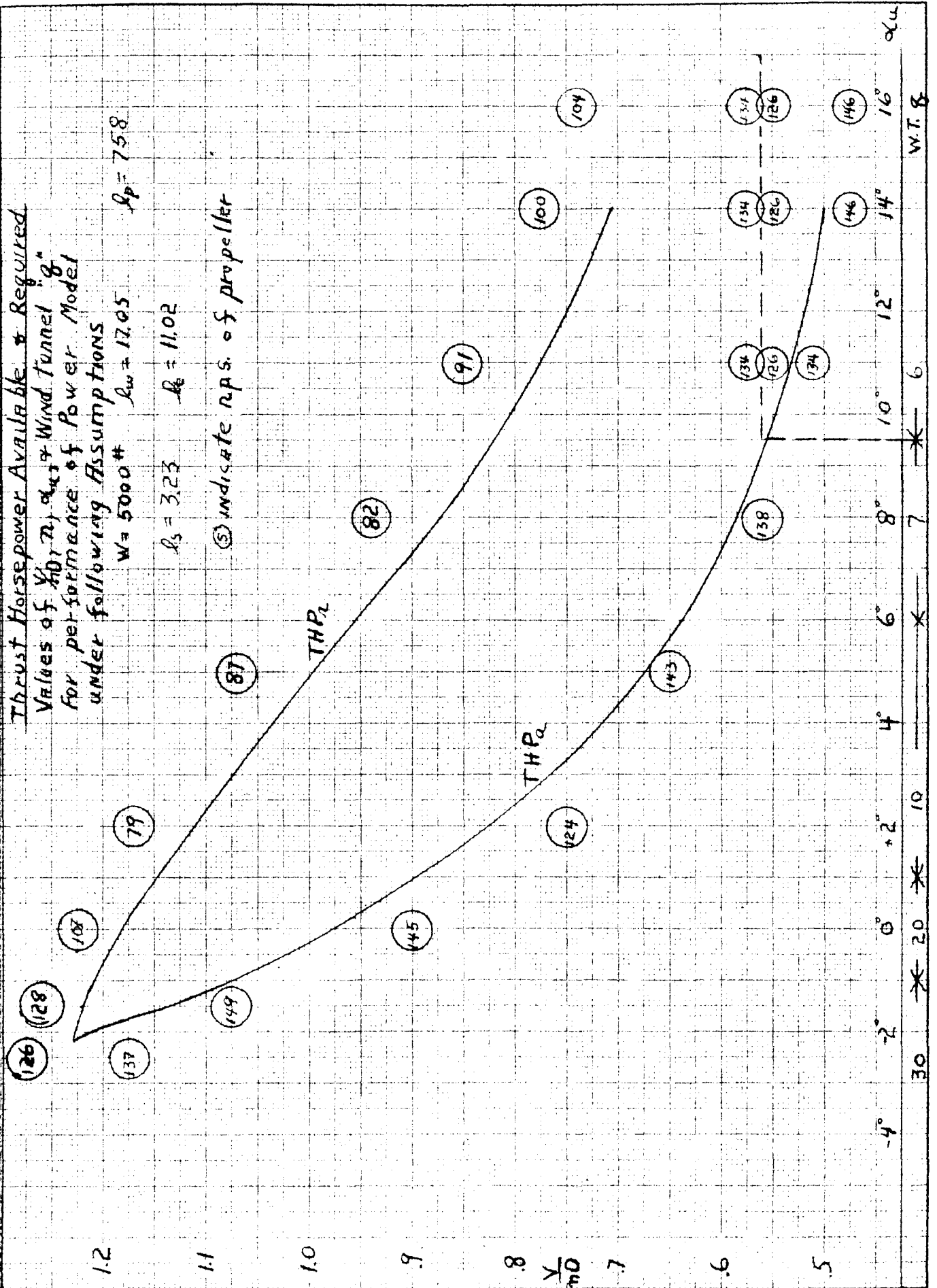


Fig. 8

of the model, assumed full scale data, aerodynamic and performance parameters.

The variation of r.p.m. with velocity was taken from N.A.C.A. Report No. 408. From the G.A.L.C.I.T. propulsive efficiency charts and the above report the value of η was determined as a function of velocity. Assuming constant engine torque, r.p.m. and η gave thrust horsepower available as a function of velocity.

The sea-level thrust horsepower required was evaluated as a function of velocity from the performance parameters.

A propulsive efficiency curve for the blade angle determined was then obtained experimentally from wind tunnel tests to check the accuracy of the apparatus.

Figure 7. shows the power curve obtained. These were then transformed into those shown in Figure 8. for a wind tunnel guide during the testing procedure.

This was carried out for the complete airplane and for the wing-fuselage combination. The resultant curves are shown in Figures 12 and 13.

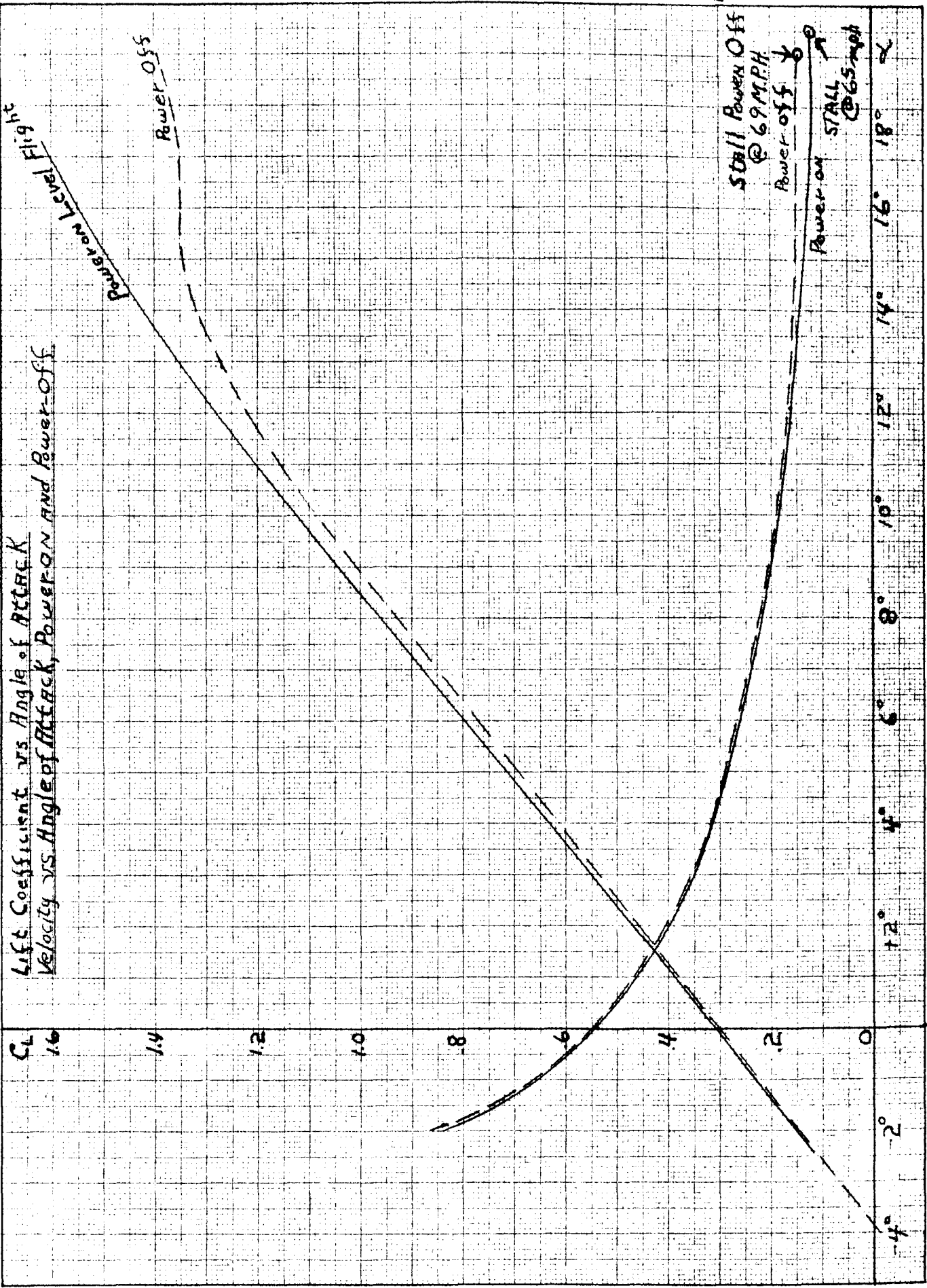
EXPERIMENTAL RESULTS

The plot of C_L vs. C_D for power on and power off is presented in Figure 10 and shows that C_{D_e} equals C_D for level flight. Therefore, "e" power on may be taken as "e" power off.

Figure 9 shows the increase in lift with power, also the velocity vs. angle of attack curves for power on and power off. The latter curves show the evident decrease in the stalling speed due to increased lift.

The plot of C_L vs. α_o of the wing-fuselage is presented in Figure 11. The increment of thrust contributing to lift is included in the curves but is very small, ranging from -0.001 at $\alpha_o = -2.08$ to $C_{L_T} = +0.0132$ at $\alpha_o = 8.07$.

Lift Coefficient vs Angle of Attack
 Velocity vs Angle of Attack, Power on and Power-off



220
 200
 180
 160
 140
 120
 100
 80
 60
 40

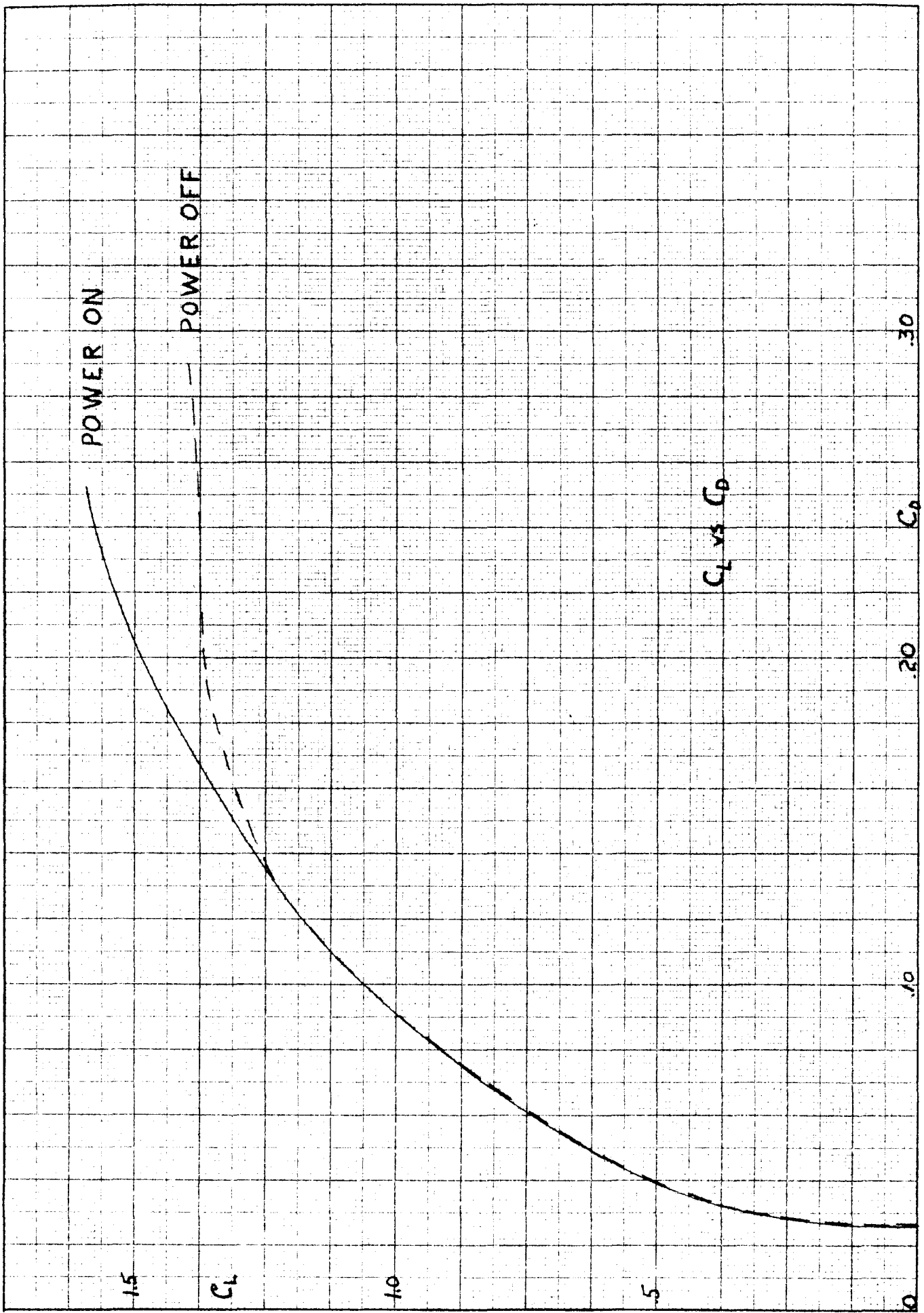


Fig. 10

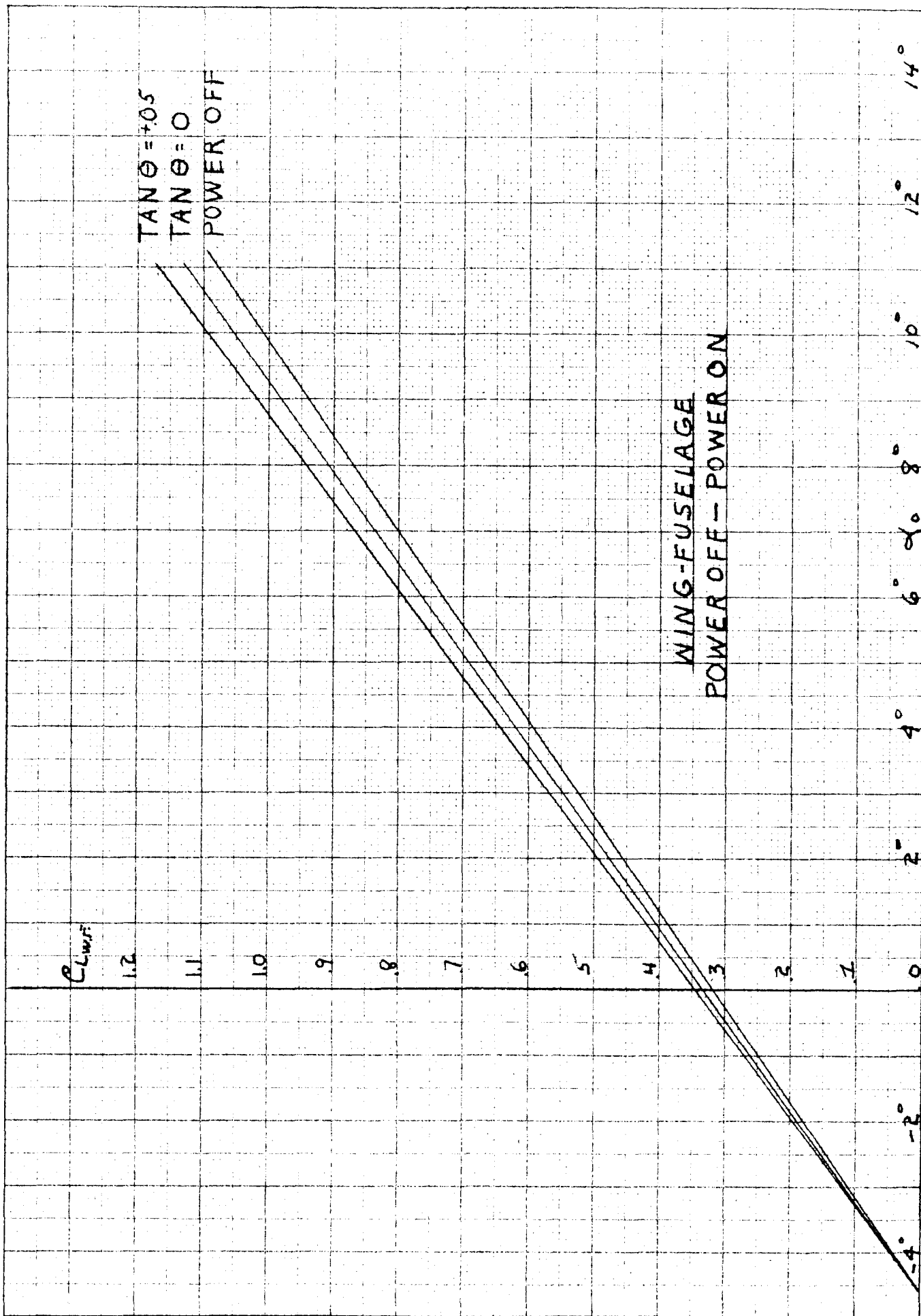
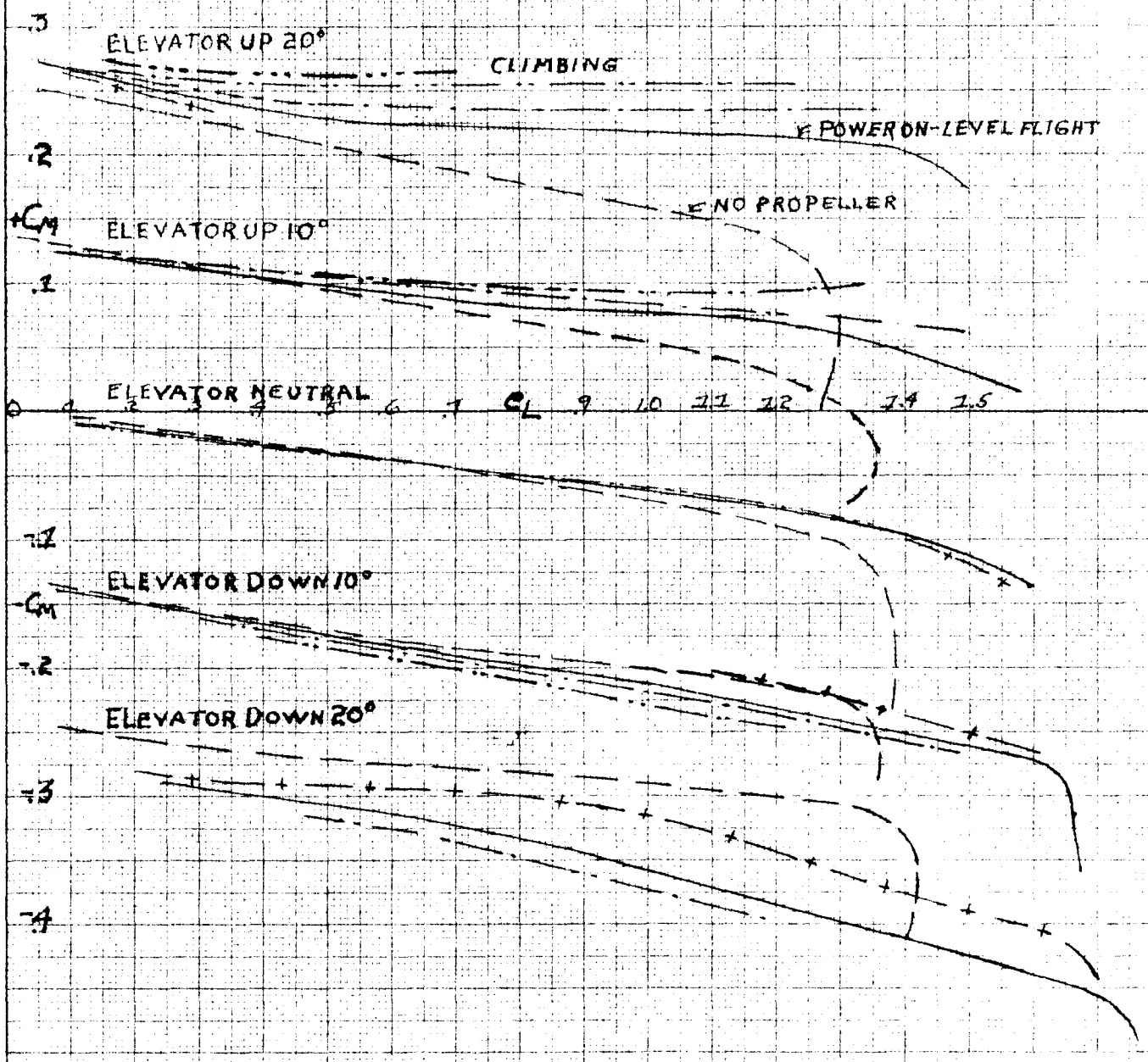


Fig. 11.

CHANGE OF MOMENT WITH POWER



LEGEND

— NO PROPELLER

--- TAN $\theta = 0$

... $\theta = +0.05$ - CLIMBING

--- " $= +0.10$

--- " $= +0.15$

-+ " $= -0.05$ - GLIDING

$\theta =$ ANGLE OF CLIMB

Fig. 12

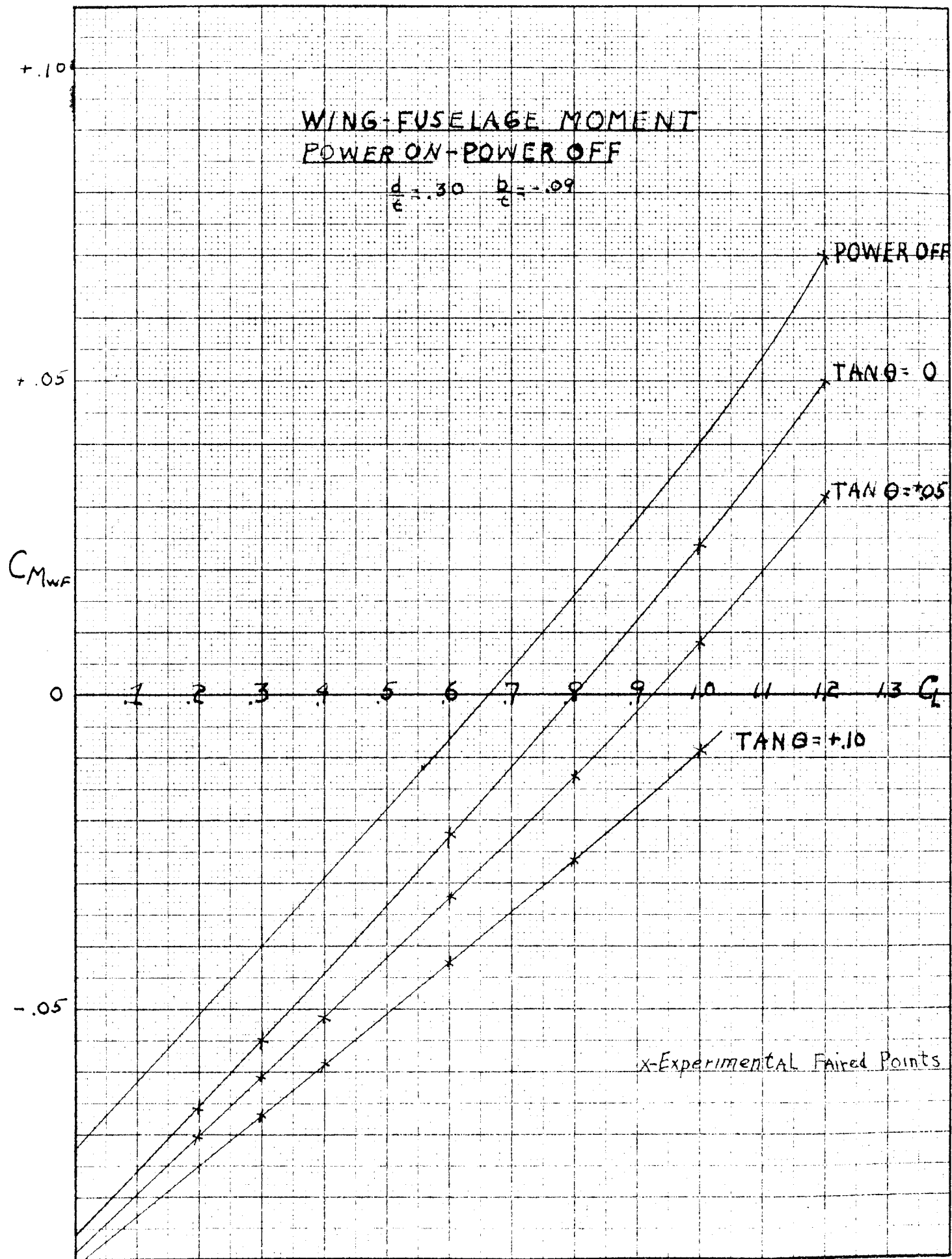


Fig. 13.

INVESTIGATION OF EXPERIMENTAL RESULTS

The presentation of the change in moment of the wing-fuselage combination with power did not seem to present any great difficulty.

The presentation of the change in the moment of the tail with power was more complicated because any normal method of presentation would have to contain C_L as an additional function, and this should be avoided if possible.

The author decided that the discussion on Page 11 showed the possible adaptation of the tail efficiency as the most likely method of obtaining results that would be independent of C_L and whose percentage changes would be applicable to any configuration of a low winged monoplane.

The power effect was divided into three classes.

- 1) Percentage change in moments of the wing-fuselage due to power.

$$\frac{\Delta C_{M_{WF}}}{C_{M_{WF_0}}} \sim f(\theta) \quad (\text{where } C_{M_{WF}} \text{ is } C_{M_{WF}} \text{ at } C_L = 0)$$

$$\frac{\Delta \frac{dC_{M_{WF}}}{dC_L}}{\frac{dC_{M_{WF_0}}}{dC_L}} \sim f(\theta)$$

Evaluating $\Delta C_{M_{WF}}$ in $C_{M_{WF_P}} = C_{M_{WF_0}} + \Delta C_{M_{WF}}$

- 2) Percentage change in moments of the tail due to power.

$$C_{M_t} = -\eta_t A C_L + B \eta_t$$

$$\text{where } A = \frac{\rho S_c'}{c S_w} \left[\frac{1 - \frac{a_0}{\pi A_w}}{1 + \frac{a_0}{\pi A_b}} \right]$$

$$B = \left[\frac{\rho S_c'}{c S_w} \left(\frac{a_0}{1 + \frac{a_0}{\pi A_b}} \right) \right] \alpha_d$$

But $\eta_t = -\frac{1}{A} \frac{dC_{M_t}}{dC_L}$ and can be evaluated from C_{M_t} vs. C_L

A may vary with power, but if A is considered constant any change may be included in $\Delta \eta_t$.

$$C_{M_{tP}} = -\eta_{tP} A C_L + \eta_{tP} B_P \quad (\text{Power on})$$

$$C_{M_{t0}} = -\eta_{t0} A C_L + \eta_{t0} B_0 \quad (\text{power off})$$

$$C_{M_{tP}} = C_{M_{t0}} - A C_L \Delta \eta_t + \eta_{tP} B_P - \eta_{t0} B_0$$

But $C_{M_{t0}}$ is measured in W.T.T.

B may vary with power on.

A is known (any change is included in $\Delta \eta_t$).

$\Delta \eta_t = \eta_{t0} - \eta_{tP}$ (η_{t0} is measured in W.T.T.)
 $\eta_{t0} B_0$ IS VALUE OF $C_{M_{t0}}$ AT $C_L = 0$ (FROM W.T.T.)
 $\therefore \eta_{tP} B_P$ and η_t are needed and can be evaluated
 from power model experiments.

3) Increment of moment due to thrust.

EXPERIMENTAL PROCEDURE AND ANALYSIS

WIND TUNNEL TESTING

Power off runs

1. $e = 0^\circ; \delta = +2^\circ$ complete airplane
2. $e = +10^\circ; \delta = +2^\circ$ " "
3. $e = +20^\circ; \delta = +2^\circ$ " "
4. $e = -10^\circ; \delta = +2^\circ$ " "
5. $e = -20^\circ; \delta = +2^\circ$ " "
6. " " *LESS TAIL SURFACES*

Power on runs (as given on Page 13.)

1. Same as 1 for power off
2. Same as 2 " " "
3. Same as 3 " " "
4. Same as 4 " " "
5. Same as 5 " " "
6. Same as 6 " " "

Use of W.T. data

- a) $\tan \theta$, C_L , α_0 , C_M , C_D , C_{D_e} , C_R were calculated.
- b) C_M vs. C_L was plotted for all runs -- power on and power off.
- c) Curves of constant $\tan \theta$ were faired through experimental points on C_M vs. C_L .
- d) For C_L values at every .1 interval, values of C_M and $\tan \theta$ were tabulated.
- e) For same value of C_L the value of C_M (wing-fuselage) was subtracted from C_M (complete airplane) for same condition of power ($\tan \theta$). This gave value of C_{M_e} for same power conditions at various values of "e".
- f) C_{M_e} vs. C_L for same "e" and various power conditions was plotted (Figure 15).
- g) From $\eta_c = -\frac{dC_{M_e}}{dC_L} \left(\frac{1}{\frac{\rho S t}{2 S_w} \left(\frac{1 - \frac{\alpha_0}{\pi AR_0}}{1 + \frac{\alpha_0}{\pi AR_0}} \right)} \right)$ the values of η_c were calculated and variation of η_c , i.e., $\frac{\eta_{c_0} - \eta_{cp}}{\eta_{c_0}}$ was plotted vs. $\tan \theta$ and ΔC_{M_e} (Figure 16).

Elimination of thrust from moment

h) Since $C_R = C_T - C_{D_e}$

AND $C_{D_e} = C_D$

Then

$$C_R = C_T - C_D$$

$$\therefore C_T = C_R + C_D$$

Also $\tan \theta = -\frac{C_R}{C_L}$

But C_R and C_D are known from W.T.T.

$\therefore C_T$ is known.

Define

$$T = C_T \frac{\rho}{2} V^2 S'$$

$$M_T = C_{M_T} \frac{\rho V^2}{2} S' t$$

and

$$M_T = T \times \text{HM} = T F$$

$$\therefore C_{M_T} = C_T \frac{F}{t}$$

TAIL MOMENT VARIATION WITH POWER

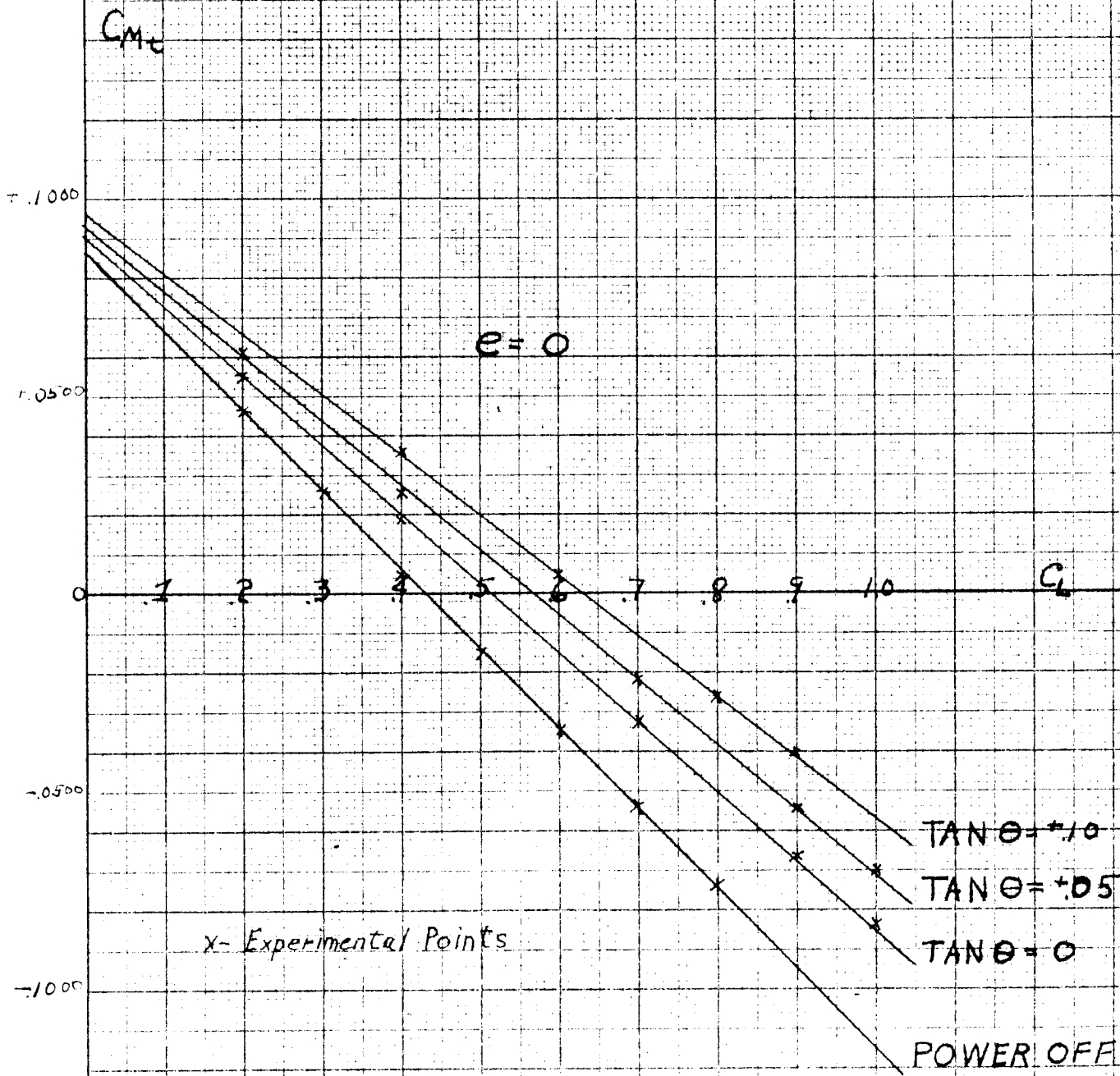


Fig. 14

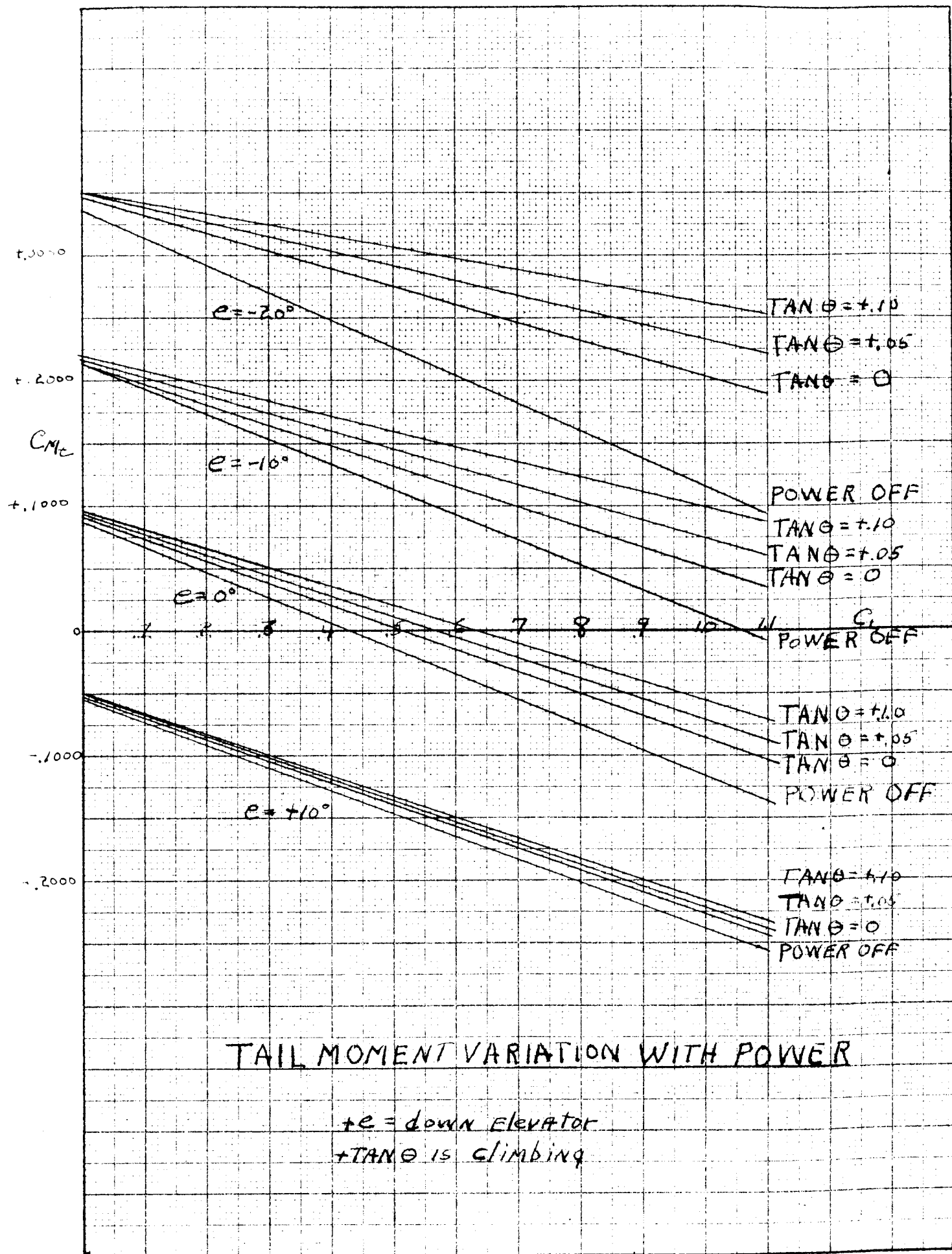


Fig. 15

VARIATION OF TAIL EFFICIENCY

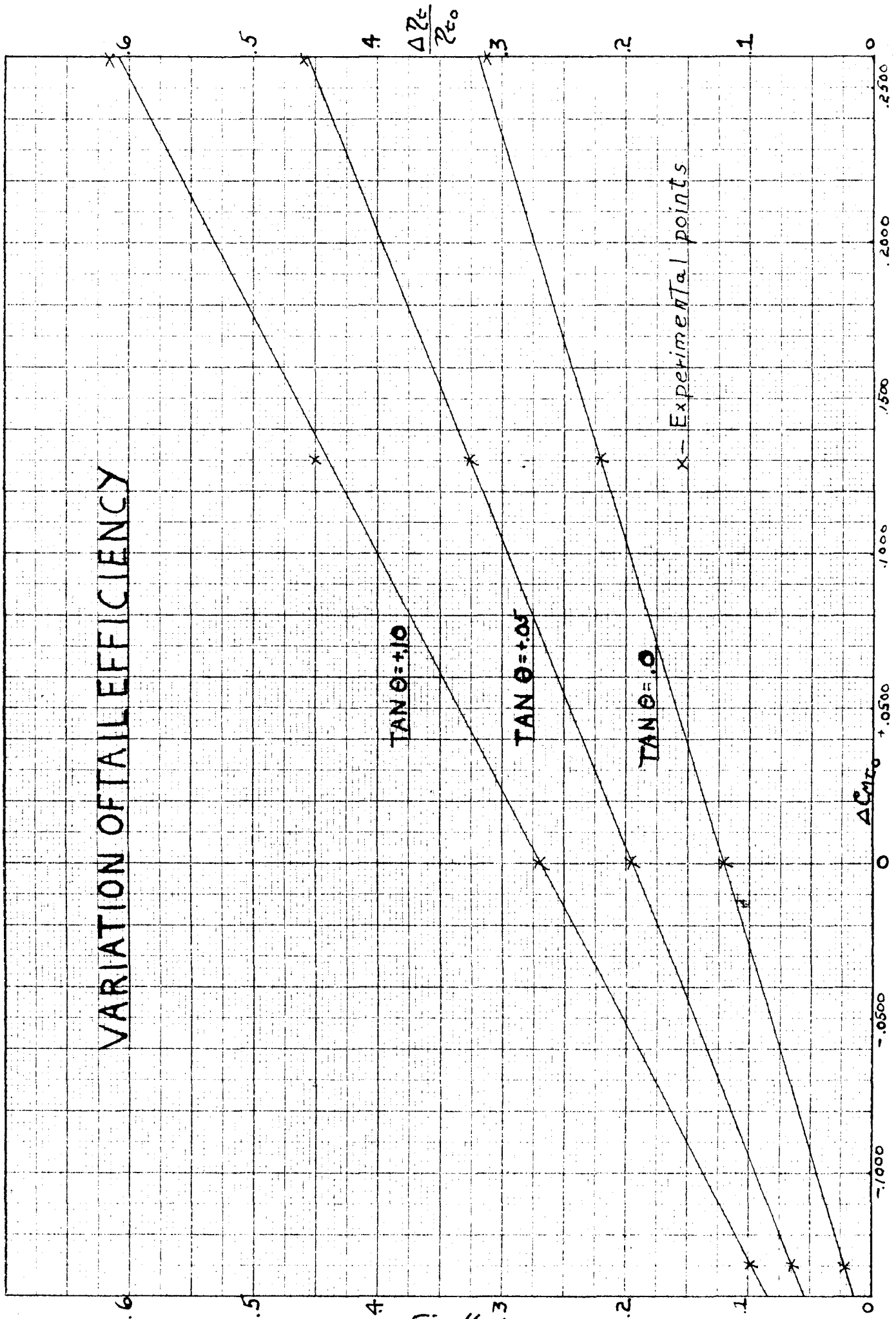


Fig. 16

WING-FUSELAGE

CHANGE IN MOMENT WITH POWER
(LESS INCREASE DUE TO THRUST)

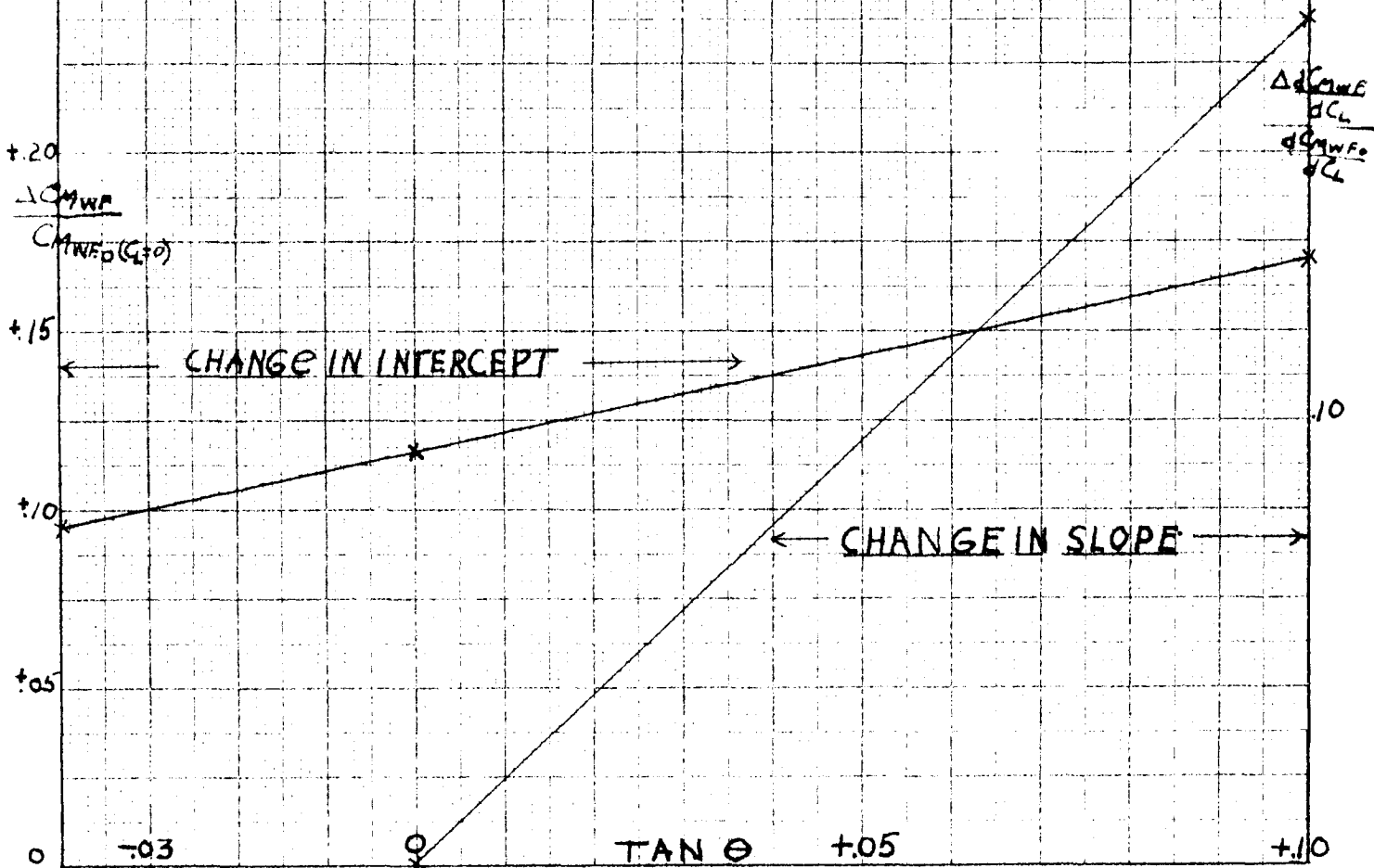
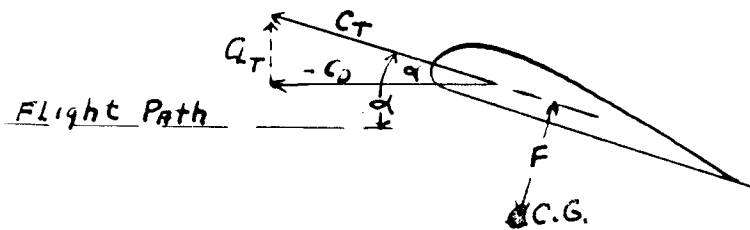


Fig. 17



Horizontal comp. of thrust must equal resultant drag

$$\therefore C_T \cos \alpha = C_R + C_D$$

$$\text{or } C_T = \frac{C_R + C_D}{\cos \alpha}$$

$$C_{M_{\text{thrust}}} = \left(\frac{C_R + C_D}{\cos \alpha} \right) \frac{F}{c}$$

For model

$$\frac{F}{c} = .09$$

- i) In plot of $C_{M_{w/F}}$ vs. C_L moment due to thrust was calculated and subtracted from $\Delta C_{M_{w/F}}$ due to power (Figure 13A), giving $\Delta C_{M_{w/F}}$ less thrust increment. This new $\Delta C_{M_{w/F}}$ due primarily to increase in velocity was plotted and the change in slope and intercept plotted in Figure 17
- j) Figures 9, 10, 11 were plotted for change in C_L and C_D , (complete airplane), C_L vs. α (wing-fuselage).

CONCLUSIONS

- 1) The addition of power is destabilizing (statically).
- 2) The destabilization is definitely dependent upon the area of wing and tail exposed to slip stream.
- 3) Destabilization caused by the tail varies with vertical position of tail with reference to M.A.C. chord of wing.

- 4) The change in moment due to thrust must be calculated.
- 5) Investigation of low-winged monoplane without tail and with various air-foil sections of same span, chord, etc., to compare $\Delta C_{H_{w.F.}}$ with Clark Y as used in this investigation.
- 6) Construction of similar charts for high winged monoplane from data of G.A.L.C.I.T. Report 148, published in Vol.3, No. 3, J. of I.A .S. is desirable.
- 7) Evaluation of M_U (power on) in dynamic stability from this report and G.A.L.C.I.T. Report 148 should be attempted.
- 8) Flight testing of all planes when time permits; for further checking of the charts presented in this report. At present there is very little flight test data available.

PART TWO

I

The calculation of the effect of power upon Longitudinal Static Stability
has been divided into three general steps.

- a) Change in the wing-fuselage moment curve due to increase in velocity.
- b) Moment due to thrust.
- c) Change in the tail moment curve due to addition of power.

II

CORRECTION OF WING-FUSELAGE MOMENT CURVE

It is to be noted in the plot of lift versus angle of attack that the increment of lift increases with angle of attack. Now at angles of attack below zero the thrust will tend to decrease, rather than increase the lift. However, the chart shows an increase of the increment of lift with angle of attack. Actual calculations of the contribution of lift due to thrust shows it to be very small compared to increment due to increase in velocity. From the above considerations it is apparent that the area of the wing exposed to the slipstream must enter directly into the increase of moment due to increase of velocity with power.

The suggested correction factor is

$$\left(\frac{S'_{we}/S'}{S_{we}/S} \right)$$

WHERE

PRIMES INDICATE AIRPLANE.

S'_{we} = EXPOSED AREA OF WING-FUSELAGE

which is to be multiplied by factors on Figure 17 for obtaining change in intercept and slope.

III

MOMENT DUE TO THRUST

See Page 16 of thesis for procedure.

IV

CORRECTION OF TAIL MOMENT CURVES

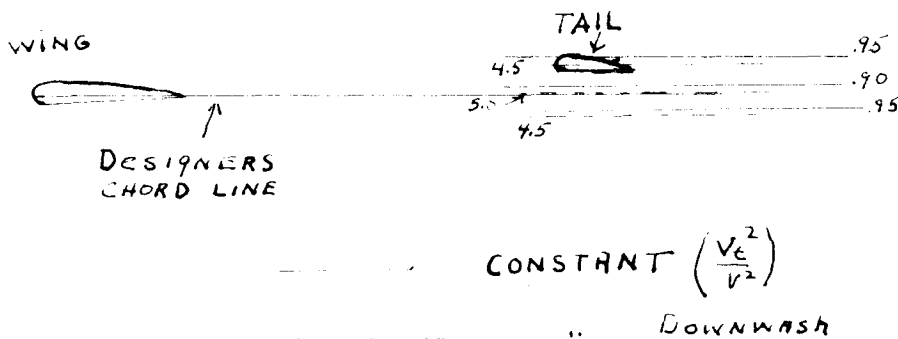
The curves Figure 15 show the change in slope and intercept with addition of power.

Fig. 16 shows $\frac{\Delta \eta_c}{\eta_{c0}} = \frac{\eta_{c0} - \eta_{cp}}{\eta_{cp}}$ vs. ΔC_{M_c} BASED UPON THE CURVES IN fig. 15.

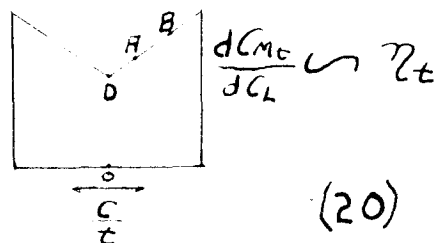
THE CHANGE IN INTERCEPT WAS SO SMALL, AND CURVES WERE EXTRAPOLATED FROM $C_L = .15$ & $C_L = 0$. Therefore this change may be neglected.

CHANGE OF SLOPE WITH VERTICAL POSITION

N.A.C.A. Report 539 shows a variation in downwash and $\frac{V_c^2}{V^2}$ with vertical position of tail for wing alone. Placing model in Figure 20 of that report shows



This variation is also shown in a W.T.T. report, which gives the following figure:



This shows that $\eta_{tB} = f\left(\frac{C_B}{c}, \frac{C_A}{c}, \eta_{tA}\right)$

$$\text{Now } \frac{\eta_{tB} - \eta_{tD}}{\eta_{tB}} = \frac{\frac{C_B}{c}}{\frac{C_A}{c}} \left(\frac{\eta_{tA} - \eta_{tD}}{\eta_{tA}} \right) \quad \text{and IF}$$

$$\left[\left| \frac{\frac{C_B}{c} - \frac{C_A}{c}}{\frac{C_A}{c}} \right| + 1 \right] \frac{\Delta \eta_{tA}}{\eta_{tA}} = \frac{\Delta \eta_{tB}}{\eta_{tB}}$$

satisfies this function, IT MAY BE USED.

Expanding gives

$$\frac{\frac{C_B}{c} - \frac{C_A}{c} + \frac{C_A}{c}}{\frac{C_A}{c}} \frac{\Delta \eta_{tA}}{\eta_{tA}} = \frac{\Delta \eta_{tB}}{\eta_{tB}}$$

$$\frac{\frac{C_B}{c}}{\frac{C_A}{c}} \frac{\Delta \eta_{tA}}{\eta_{tA}} = \frac{\Delta \eta_{tB}}{\eta_{tB}}$$

Now N.A.C.A. Report 539 shows that for tail lengths similar to model the minimum position for the tail is along the designer's chord line. Also, the **W.T.T.** report shows that the tail efficiency is a ratio of vertical height of tail above this minimum position. The model has given a position other than the minimum position and therefore any other point along the curve can be evaluated. The equation becomes

$$\left[\left| \frac{\frac{C'_t}{c} - .15}{.15} \right| + 1 \right] \frac{\Delta \eta_t}{\eta_{t_0}} = \frac{\Delta \eta_t}{\eta_{t_0}} \quad \text{FOR AIRPLANE CONSIDERED}$$

CHANGE OF SLOPE WITH EXPOSED AREA

Most modern airplanes have a $\frac{S'_{ce}}{S'_c} \doteq .70$ if the propeller diameter is drawn straight back to the tail. Similarly with the model. For this reason the entire tail is considered as being in the slipstream and correction factor similar to wing-fuselage factor becomes 1.

CHANGE OF INTERCEPT

The same correction factors will be used as for change in slope. The percentage change in intercept is from zero at $e = 0^\circ$ to .033 at up 20° , which can in general be neglected, since .0100 is equivalent to a stabilizer angle shift of ^{ABOUT} one-fourth degree.

It is apparent that the center of gravity must be shifted to the same position as the model for the wing-fuselage moment curve, power off condition, in cases where the change in slope with power is other than zero.

SUGGESTED PROCEDURE FOR CORRECTION OF POWER OFF MOMENT CURVES

DUE TO ADDITION OF POWER

a) Tabulate

R_t

R_w

S' (AREA OF WING-FUSELAGE - NACA)

S'_t (AREA OF HORIZONTAL TAIL SURFACES)

t' (AVERAGE CHORD IN FRONT OF TAIL)

C' (PERPENDICULAR DISTANCE FROM DESIGNERS CHORD LINE TO TAIL)
(HINGE LINE)

t (M.A.C.)

b/c

$\frac{h}{c}$

$\frac{d}{c}$

l

$S'_{W.F.C.}$ (AREA OF WING-FUSELAGE BEHIND PROPELLERS)

b) Plot C_{M_0} vs. C_L (Complete airplane-power off)

Plot $C_{M_{WF_0}}$ vs. C_L (power off)

c) Calculate $C_{M_{T_0}}$ vs. C_L (power off)

d) If Figure 17 shows change in slope for plot of $\frac{\Delta C_{M_{WF}}}{\Delta C_L}$ vs. $TAN \theta$,
 ROTATE C_L AXIS TO C.G. = .31 ON PLOT OF $C_{M_{WF_0}}$ VS C_L

Pick off $\frac{\Delta C_{M_{WF}}}{C_{M_{WF_0}}}$ and $\frac{\frac{\Delta C_{M_{WF}}}{\Delta C_L}}{\frac{\Delta C_{M_{WF_0}}}{\Delta C_L}}$ and multiply by factor $\frac{S_{WE}}{S}$
 .257

Correct slope and intercept of $C_{M_{WF}}$ vs. C_L

e) Calculate moment due to thrust and add to resultant of (d).

$$C_{M_{THRUST}} = \frac{C_R + C_D}{\cos \alpha} \times ARM$$

For $\tan \alpha = 0$

$$C_{M_{THRUST}} = \frac{C_D}{\cos \alpha}$$

f) For appropriate $\tan \theta$ and ΔC_{M_t} pick off $\frac{\Delta \eta_t}{\eta_{t_0}}$

$$\text{Then } \left[\left| \frac{\eta_t' - \frac{C}{c}}{\frac{C}{c}} \right| + 1 \right] \frac{\Delta \eta_t}{\eta_{t_0}} = \left(\frac{\Delta \eta_t}{\eta_{t_0}} \right)' \quad (\text{percentage correction})$$

$$\therefore \Delta \eta_t' = \eta_{t_0} \left[\left| \frac{\eta_t' - .15}{.15} \right| + 1 \right] \frac{\Delta \eta_t}{\eta_{t_0}}$$

Plot $C_{M_{T_p}}$ vs. C_L

g) Add $C_{M_{T_p}}$ vs. C_L to $C_{M_{WF_p}}$ vs. C_L to obtain

C_{M_p} vs. C_L

h) For new C.G. position needed for desired stability compute new value of tail length and repeat (f).

It must be remembered that the elevator or stabilizer angle will be in error because the model had a fixed elevator, whereas flight tests have free elevator, which changes intercept and slope of the tail moment curve.

In general, the position of the center of gravity needed for a given stability agrees within 0.01 of the flight test data available for entirely different types of airplanes than was used in the investigation.

AGREEMENT WITH FLIGHT TEST DATA

MAKE	TYPE	$\frac{dC_M}{dC_L}$	C_L (TRIM)	$\frac{d}{L}$ (C.G.)	$\delta + e \frac{F_{TS}}{TS}$	METHOD
Lockheed	2 ENGINE LOW-WING	-.10	.3	.25	0	FLIGHT
"	"	-.10	.3	.256	+1.8°	CALCULATED
"	"	-.03		.32	0	FLIGHT
"	"	-.03		.326		CAL.
"	"	.00	—		0	FLIGHT
"	"	.00	—	.356	—	CAL.
DC-2	"	-.09	.2	.20	0	FLIGHT
"	"	-.09	.2	.204	+1/4°	CAL.

TYPICAL EXAMPLE

$$\frac{S'_{we}}{S_w} = \frac{293.4}{939} = .313$$

$$\frac{C'_l}{l} = \frac{73.5 \times \cos 2^\circ}{170} = \frac{73.5}{170} = .433$$

$$\frac{b}{l} = \frac{-.4 \times 12}{142.3} = -.0565$$

$$\frac{d}{l} = .20$$

$$l = 434'' @ \frac{d}{l} = .20$$

$$AR_c = 3.48$$

$$AR_w = 7.7$$

$$i_w = +2^\circ$$

$$l(\text{MAC}) = 142.3$$

$$\text{thrust ARM} = F = 19.5''$$

$$\frac{F}{l} = \frac{19.5}{142.3} = .137$$

$$S'_c = 187 \text{ sq. ft.}$$

$$A = \frac{\rho S'_c}{l S_w} \left[\frac{1 - \frac{a_0}{\pi AR_w}}{1 + \frac{a_0}{\pi AR_c}} \right] = \frac{434 \times 181}{142.3 \times 939} \left[\frac{1 - \frac{5.5}{7.7\pi}}{1 + \frac{5.5}{3.48\pi}} \right] = .306$$

THRUST LINE 8.5" below MAC ; AND 58.5" below TAIL

TAIL MOMENT CORRECTION

FROM PLOT OF C_{M_0} vs. C_L AND $C_{M_{WF_0}}$ vs. C_L PLOT C_{M_0} vs. C_L

$$\frac{dC_{M_0}}{dC_L} = -.1830 ; \eta_{t_0} = -\frac{dC_{M_0}}{dC_L} \frac{1}{A} = \frac{.1830}{.306} = .5975$$

FROM FIG. 16 WITH $\tan \theta = 0$ AND $\Delta C_{M_0} = 0$ FIND $\frac{\Delta \eta_t}{\eta_{t_0}} = .120$

$$\Delta \eta_t = \eta_{t_0} \left[\left| \frac{C'_l - .15}{.15} \right| + 1 \right] \times .120 = .207$$

$$\eta_{cp} = \eta_{t_0} - \Delta \eta_t = .5975 - .207 = .3905$$

PLOT NEW $C_{M_{cp}}$ vs. C_L

WING FUSELAGE CORRECTION

FROM FIG. 17 $\frac{\Delta C_{M_{WF}}}{C_{M_{WF_0}}} = +.117$; $C_{M_{WF_0}}$ (FROM $C_{M_{WF_0}}$ vs. C_L) = -.0500

$$C_{M_{WF_p}} = -.0500 + (.117 \times \frac{.313}{.257} \times (-.0500)) = -.0570$$

ALSO FIG. 17 SHOWS CHANGE IN SLOPE = 0

COMPONENT OF MOMENT DUE TO THRUST.

$$C_{M_T} = C_T \times \frac{F}{l} = \frac{C_D}{\cos \alpha} \frac{F}{l}$$

C_L	C_D	$\cos \alpha$	C_T	$C_{M_T} = C_T \times .137$
0.0	.0200	1.0	.0200	.0028
.2	.0220	"	.0220	.0030
.4	.0250	"	.0250	.0034
.6	.0350	"	.0350	.0048

PLOT CORRECTIONS AND THEN $C_{M_{WF_p}} + C_{M_{cp}} = C_{M_p}$

FOR ANY DESIRED $\frac{dC_M}{dC_L}$ ROTATE C_L AXIS TO PROPER C.G. ON $C_{M_{WF}}$ vs. C_L .

